

**Power-law behavior reveals phase transitions in landscape controls of fire regimes****Donald McKenzie<sup>1</sup>****Maureen C. Kennedy<sup>2</sup>****<sup>1</sup>Pacific Wildland Fire Sciences Lab, US Forest Service****<sup>2</sup>School of Forest Resources, University of Washington**

**Summary: In low-severity fire regimes of the American West and elsewhere, landscape memory of fire events is registered in fire-scarred trees, with temporal record lengths often exceeding 200 years<sup>1-5</sup>. Understanding the environmental controls on historical wildfires, and how they changed across spatial scales, is difficult because there are no surviving explicit records of either weather or vegetation (fuels). We show how power laws associated with fire-event time series arise in limited domains of parameters that represent critical transitions in the controls on landscape fire. We used stochastic simulations iteratively with Monte Carlo inference to replicate the spatio-temporal structure of historical fire-scar records in forested watersheds of varying topographic complexity. We find that the balance between endogenous and exogenous controls on fire spread shifts with topographic complexity, where in the most complex landscapes the endogenous controls dominate and the pattern exhibits criticality. Comparison to a self-organized criticality (SOC) model<sup>6,7</sup> shows that the latter mimics historical fire only in a limited domain of criticality, and is not an adequate mechanism to explain landscape fire dynamics, which are shaped by both endogenous and exogenous controls. Our results identify a continuous phase transition in landscape controls,**

**marked by power laws, and provide an ecological analogue to critical behavior in physical and chemical systems<sup>8-11</sup>. This explicitly cross-scale analysis provides a paradigm for identifying critical thresholds in landscape dynamics that may be crossed in a rapidly changing climate.**

Nature displays power laws in frequency distributions of diverse phenomena<sup>10</sup> and critical exponents associated with phase transitions<sup>11</sup>. The latter are well known in thermodynamic and other physical systems but have been addressed only qualitatively in ecological systems<sup>8,12</sup>. For example, environmental controls on wildfires are thought to cross thresholds between fine-scale endogenous controls such as topography and spatial patterns of fuels and broader-scale drivers such as climate. We use stochastic simulation and cross-scale analysis to quantify these thresholds in historical fire regimes.

Fire-scarred trees provide a deep temporal record of fire activity in low-severity fire regimes<sup>1,13</sup> wherein most trees survive, and record, most fires. We use this full spatio-temporal record to identify phase transitions in landscape fire between domains of endogenous vs. exogenous control. The core of our analysis is a variogram-like metric whose scaling behavior follows power laws only when the fire regime is at a critical point. We provide an alternative interpretation of spatial patterns of fire to that of self-organized criticality (SOC) and other theories that do not adequately incorporate heterogeneous landscape controls on fire.

We use a spatially explicit fire-history database (Figure 1) with more than 7000 fire-scarred trees. We replace the gamma statistic (semivariance) in a variogram with the

Sørensen's distance<sup>2</sup> (SD), a multivariate measure of dissimilarity between pairs of time series of fires recorded in fire scars. The expectation of the SD variogram can be derived analytically from simple stochastic properties of fire spread and its memory in fire-scarred trees (SI). Power-law behavior is evident in SD variograms from the most topographically complex watersheds, but clearly not in those with more simple topography (Figure 2). We deconstruct this power-law behavior with a stochastic model whose output replicates the SD variograms for each watershed.

We use a raster model of fire spread<sup>3</sup> with three control parameters:  $p_{\text{spread}}$  = the global probability that a cell burns after a neighboring cell has burned,  $p_{\text{scar}}$  = the probability that a recorder tree in the cell records the fire, and  $\mu_{\text{size}}$  = the average maximum size a fire could attain (where individual fire sizes in the simulated fire history are drawn from a probability distribution with mean =  $\mu_{\text{size}}$ ).  $p_{\text{spread}}$  represents an endogenous control on fire spread, e.g., the availability of fuel or a topographic barrier, and  $\mu_{\text{size}}$  represents an exogenous control, e.g., the maximum duration of fire-conductive weather. The parameter  $p_{\text{scar}}$  is the likelihood a tree that experiences fire records it with a scar, and fire spread is independent of this scarring probability.

We found a percolation threshold for  $p_{\text{spread}}$ , which is the value of  $p_{\text{spread}}$  at which absent a size constraint, the first fire spans a suitably large raster grid. For our system we estimate this first fire spans at  $p_{\text{spread}} = 0.495$ . When we vary  $p_{\text{spread}}$  between 0.35 and 1.0 and remove the size constraint, we find two domains in which simulated SD variograms follow power laws (Figure 3), one of which is centered on the percolation threshold, and represents a transition between fires that are mostly small and cannot propagate across a

landscape and larger ones that can. This characterizes a phase transition in landscape dynamics over a narrow range of values for the parameter  $p_{\text{spread}}$ , suggesting a region of criticality<sup>8,13</sup> because within it the SD variograms follow power laws.

In the watersheds with the most complex topography, values of  $p_{\text{spread}}$  that produce simulated SD variograms indistinguishable from the observed are very close to the percolation threshold, within the domain found to produce power-law SD variograms (Figure 4a). The  $\mu_{\text{size}}$  parameter for these landscapes is ill-defined (Figure 4b), as simulated fires fail to spread before the randomly drawn fire size is reached so the simulated dynamics are independent of the value of  $\mu_{\text{size}}$ . The analog to  $p_{\text{spread}}$  could be a topographic barrier or a discontinuity of fuels, and we interpret that for landscapes with  $p_{\text{spread}}$  near the percolation threshold there is a balance between exogenous and endogenous controls on fire spread.

In contrast, as topographic complexity lessens, the distribution of  $p_{\text{spread}}$  values able to replicate observed SD variograms converges well above the percolation threshold (Figure 4a). The  $\mu_{\text{size}}$  parameter is well defined for these landscapes because the simulated fires require the random fire size stopping rule in order to not span the raster grid (Figure 4b). For  $p_{\text{spread}}$  well above the percolation threshold changes in the  $p_{\text{spread}}$  parameter have diminished effects and the shape of the SD variogram is more sensitive to changes in the  $\mu_{\text{size}}$  parameter, such that the balance is tilted toward exogenous controls.

We next ask whether a self-organized criticality (SOC) model, which has been proposed to explain power laws in fire-size distributions<sup>7</sup>, can replicate the observed variability in the SD variograms. We built a simple “forest fire” model<sup>6</sup> but added a CSR

pattern (complete spatial randomness) of simulated recorder trees as in our original model. The SOC model is said to depend solely on emergent system properties, which self-organize to a critical state independently of exogenous driving forces. By tuning the ratio of frequency of ignitions to fuel accumulation, as in the original SOC model<sup>6</sup>, we sought to replicate the observed SD variograms in the two watersheds with the most contrasting topographic complexity: Swauk Creek and Twenty Mile. We find that whereas the SOC model can replicate the spatial structure (and power-law behavior) recorded in the SD variogram for Swauk Creek, with complex topography, in the watershed with the simplest topography (Twenty Mile) it does not (Figure 4c).

We draw two inferences from this. First, SOC cannot predict the scaling region surrounding the phase transition we discovered and explained with our model; second, SOC is therefore an incomplete representation of processes that drive real fire regimes across landscapes except perhaps at precisely the parameter values where dynamics are in a domain of criticality. Furthermore, it is even less likely that SOC is globally justified as a mechanism for fire-size distributions across an entire region<sup>14</sup>, where fires do not experience the same environmental controls, nor do they influence each other's behavior and spread.

The underlying assumption of SOC is that the endogenous processes controlling fire on real landscapes operate in a region of criticality. Not surprisingly then, the dynamics of SOC overlap with our model near the percolation threshold (also a region of criticality). We show that this region applies to watersheds with complex topography, but not to watersheds with simpler topography. Unlike SOC, our model finds a transition

between sites where the endogenous controls (e.g., topographic constraints) balance exogenous forcings (e.g., fire weather)<sup>15</sup> and sites where exogenous forcings have a greater impact. Although SOC may indeed be a mechanism producing power-law behavior<sup>9</sup>, on real landscapes it operates only within the phase transition we have identified. A further inference is that the SD variogram not only provides more information about historical fires than (reconstructed) fire-size distributions, but also is a more sensitive and robust indicator of criticality<sup>8</sup>.

Universal explanations are rare in ecological phenomena. They generally fail to be consistent with observations except in limited domains. Our simple stochastic model, in conjunction with scaling laws as manifest in the SD variogram, has identified a scaling region with strong parallels to phase transitions in the physical sciences, but the difference is that this domain of criticality is embedded in complex causal dependencies characteristic of ecological systems<sup>16</sup>. For example, our phase transition is fairly abrupt in units of the stochastic parameter  $p_{\text{spread}}$ , but spans a broader scaling region in more standard units of topographic complexity, e.g., fractal dimension. The strength of power-law behavior in the observed SD variograms (Figure 2) is strongly correlated with the estimated fractal dimensions of the watersheds<sup>2,17</sup>. We would expect this scaling region to shift with stronger exogenous forcing, such as the increased flammability and more intense fire behavior in a hotter drier climate. Under such conditions topography would have to be even more complex for fire dynamics to remain at the phase transition.

Quantifying the transition between endogenous and exogenous controls on landscape fire should improve predictions of the response of fire regimes to a rapidly

changing climate<sup>4,18</sup>. The power-law domain in SD variograms is a surrogate for the interactions of multiple processes at criticality (e.g., fire weather, topographic constraints and their effect on fuel configurations, tree scarring by fire), all of which can be measured only with considerable error and whose future patterns are uncertain. Future climate may sharpen the delineation between endogenous and exogenous controls at those sites at criticality, where more extreme weather effectively increases  $p_{\text{spread}}$ , or overcomes the limits imposed with lower  $p_{\text{spread}}$  (moves the system away from the phase transition). By overlaying barriers to fire spread at judiciously chosen coordinates<sup>19</sup> to mimic increasing topographic complexity, we may discover simple but robust treatments to maintain fire-adapted landscapes that are resilient to climate change.

### Methods Summary

We used the neutral model to produce simulated SD variograms and evaluated how well it can replicate the observed SD variograms using a Monte Carlo goodness-of-fit procedure<sup>20</sup>, which tests the hypothesis: is the observed pattern a typical model realization? For each site this procedure returns the set of combinations of  $p_{\text{spread}}$ ,  $p_{\text{scar}}$ , and  $\mu_{\text{size}}$  that cannot be rejected relative to the observed pattern. We used an analogous procedure to evaluate the SOC model, finding the combinations of frequency of sparks ( $f$ ) and probability of scarring ( $p_{\text{scar}}$ ) that cannot be rejected. A significance level of 0.25 was set for both.

To quantify the region of criticality, we evaluated domains of  $p_{\text{spread}}$  over which the neutral model produces power-law SD variograms. First we sampled 1000 values of

$p_{spread}$  uniformly on (0,1). We set the simulation model to remove the size-based stopping rule, thereby isolating the effect of  $p_{spread}$  on the shape of the SD variogram. For each value of  $p_{spread}$  we conducted 20 replicate simulations, yielding 20 simulated SD variograms for each value of  $p_{spread}$ . We then used the replicate simulations in an F-test for lack-of-fit to determine if the power-law can be rejected for the simulated SD variograms with the associated value of  $p_{spread}$ . The significance level was 0.10.



## References

1. Falk, D. A., Miller, C., McKenzie, D., & Black, A. E. Cross-scale analysis of fire regimes. *Ecosystems* **10**, 809-823 (2007).
2. Kellogg, L.-K. B., McKenzie, D., Peterson, D. L., & Hessler, A. E. Spatial models for inferring topographic controls on historical low-severity fire in the eastern Cascade Range of Washington, USA. *Landscape Ecol.* **23**, 227-240 (2008).
3. Kennedy, M. C., & McKenzie, D. Using a stochastic model and cross-scale analysis to evaluate controls on historical low-severity fire regimes. *Landscape Ecol.* **25**, 1561-1573 (2010).
4. Falk, D. A., *et al.* Multiscale controls of historical forest fire regimes: new insights from fire-scar networks. *Frontiers Ecology Environ.* doi:10.1890/100052 (2011).
5. Swetnam, T. L., Falk, D. A., Hessler, A. E., & Farris, C. Reconstructing landscape pattern of historical fires and fire regimes. In McKenzie, D., Miller, C., & Falk, D. A. (eds) *The Landscape Ecology of Fire* (Springer, Dordrecht, The Netherlands, 2011).
6. Drossel, B., & Schwabl, F. Self-organized critical forest-fire model. *Phys. Rev. Lett.* **69**, 1629-1632 (1992).
7. Malamud, B. D., Morein, G., & Turcotte, D. L. Forest fires: an example of self-organized critical behavior. *Science* **281**, 1840-1842 (1998).
8. Pascual, M., & Guichard, F. Criticality and disturbance in spatial ecological systems. *Trends Ecol. Evol.* **20**, 88-95 (2005).
9. Brown, J. H., *et al.* The fractal nature of nature: power laws, ecological complexity, and biodiversity. *Phil. Trans. Royal Soc. B* **357**, 619-626 (2002).

10. Newman, M. E. J. Power laws, Pareto distributions, and Zipf's law. *Contemp. Physics* **46**, 323-351 (2005).
11. Binney, J. J., Dowrick, N. J., Fisher, A. J., & Newman, M. E. J. *The Theory of Critical Phenomena* (Oxford Science Publications, Oxford, UK, 1992).
12. Roy, M., Pascual, M., & Franc, A. Broad scaling region in a spatial ecological system. *Complexity* **8**, 19-27 (2003).
13. Hessler, A. E., McKenzie, D., & Schellhaas, R. Drought and Pacific Decadal Oscillation linked to fire occurrence in the inland Pacific Northwest. *Ecol. Appl.* **14**, 425-442 (2004).
14. Malamud, B. D., Millington, J. D. A., & Perry, G. L. W. Characterizing wildfire regimes in the United States. *Proc. Nat. Acad. Sci. USA* **102**, 4694-4699 (2005).
15. Boer, M., Sadler, R. J., Bradstock, R. A., Gill, A. M., & Grierson, P. F. Spatial scale invariance of southern Australian forest fires mirrors the scaling behaviour of fire-driving weather events. *Landscape Ecol.* **23**, 899 (2008).
16. Mitchell, S. D. *Unsimple Truths: Science, Complexity, and Policy* (U. Chicago Press, Chicago, 2009).
17. McKenzie, D., Kellogg, L.-K. B., Miller, C., Falk, D. A., & Black, A. E. Scaling laws and fire-size distributions in historical low-severity fire regimes. *Geophysical Research Abstracts*, **8** (2006).
18. McKenzie, D., Miller, C., & Falk, D. A. Toward a theory of landscape fire. In McKenzie, D., Miller, C., & Falk, D. A. (eds) *The Landscape Ecology of Fire* (Springer, Dordrecht, The Netherlands, 2011).

19. Finney, M. Design of regular landscape fuel treatment patterns for modifying fire growth and behavior. *For. Sci.* **47**, 219-227 (2001).
20. Waller, L. A., Smith, D., Childs, J. E., & Real, L. A. Monte Carlo assessments of goodness-of-fit for ecological simulation models. *Ecol. Modell.* **164**, 49-63 (2003).

**Acknowledgements** We thank C. Miller, P.F. Hessburg, M.A. Moritz, and D.L. Peterson for helpful reviews of an earlier version, R.A. Norheim for cartography, and the Pacific Northwest Research Station, US Forest Service, for financial support.

**Author Contributions** D.M. and M.C.K. contributed equally to the paper. D.M. compiled the fire-history data, designed the study, and led the writing. M.C.K. performed modeling and analysis. D.M. and M.C.K. interpreted results.

**Author Information** The authors declare no competing financial interests. Correspondence and requests for materials should be addressed to D.M. (e-mail: [dmck@uw.edu](mailto:dmck@uw.edu)) or M.C.K. (e-mail: [mkenn@uw.edu](mailto:mkenn@uw.edu)).

## Figure legends

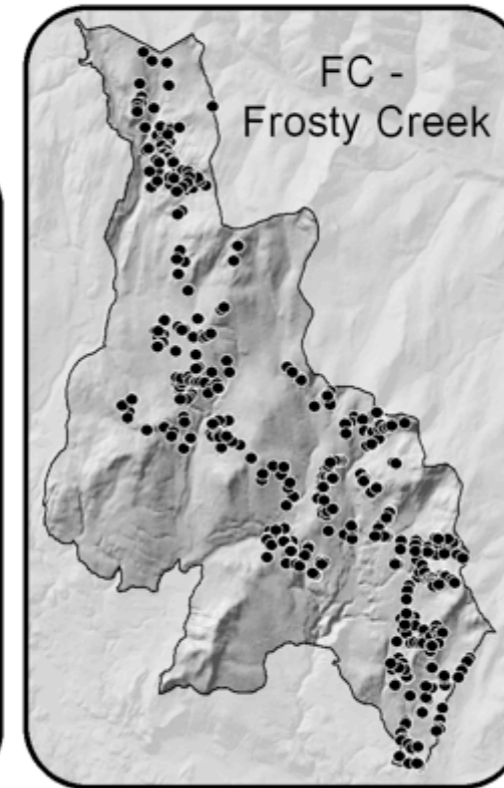
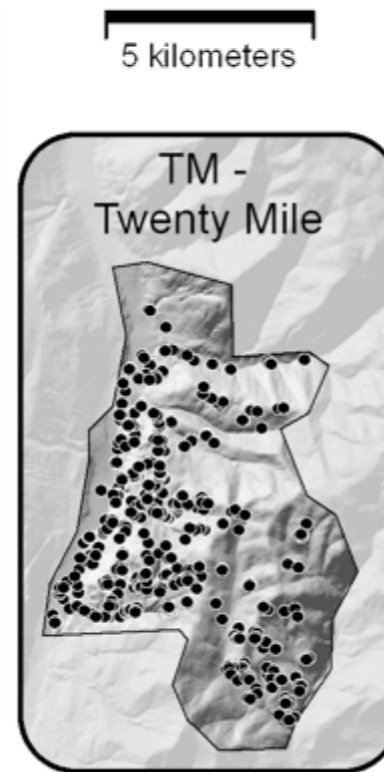
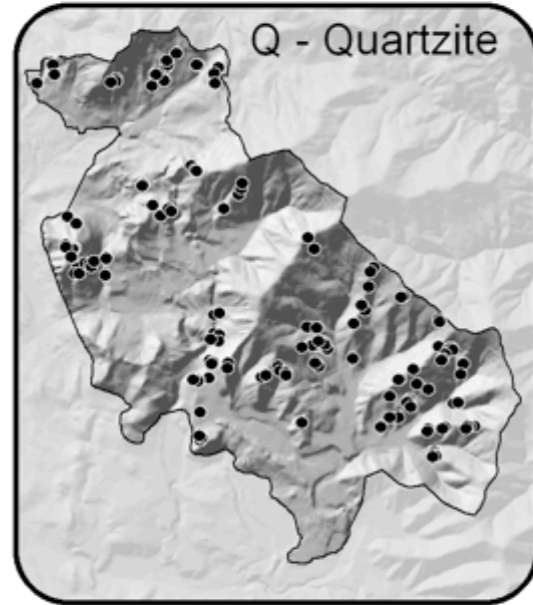
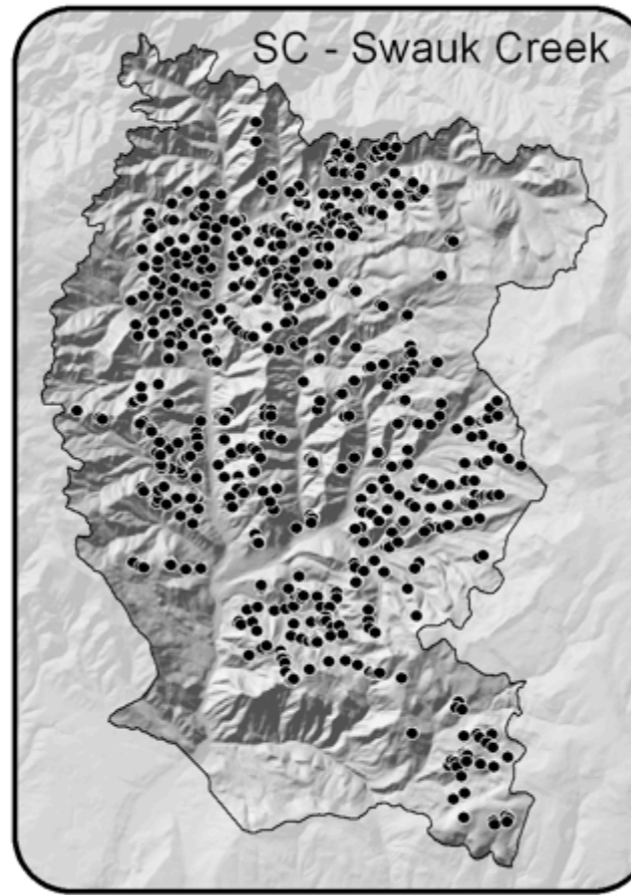
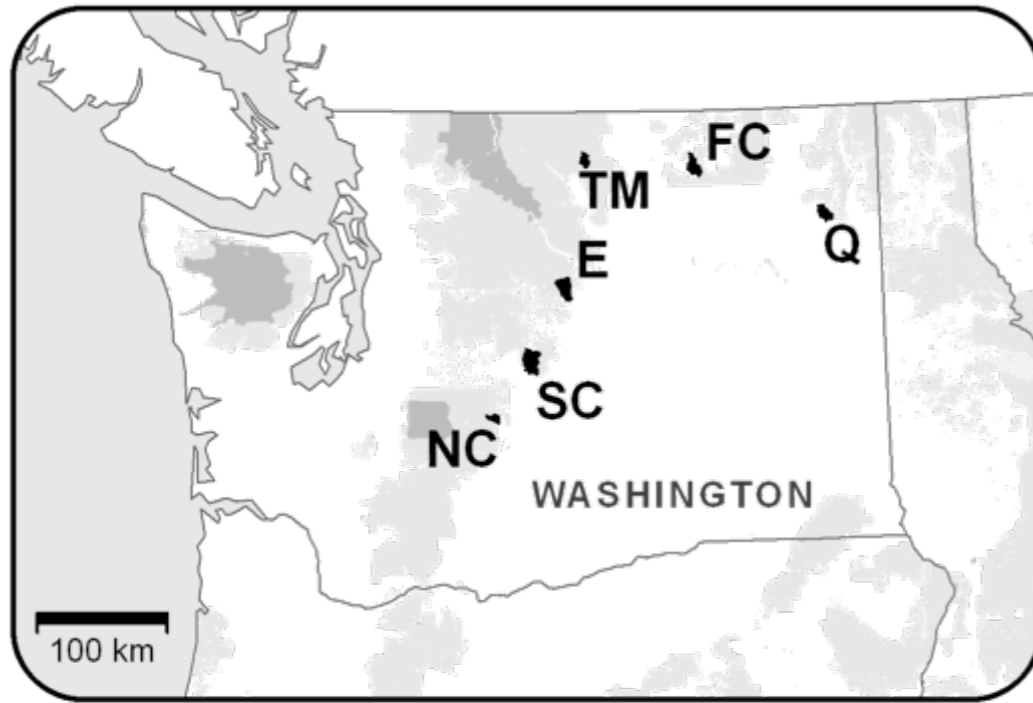
**Figure 1:** Spatially explicit fire-scar records distributed across semi-arid mountain ecosystems of Washington state, USA. Each point represents an individual recorder tree. The record extends back to the 1500s, but most trees in the database recorded a fire by 1700, and there were few fires after 1900, marking the onset of fire exclusion. We therefore used only data from 1700-1900 in this analysis. Fractal dimensions for each watershed (2 - Hurst exponent from roughness-length regressions<sup>2</sup>) are Twenty Mile (1.20), Frosty Creek (1.25), Entiat (1.30), Nile Creek (1.33), Quartzite (1.35), Swauk Creek (1.40).

**Figure 2:** Increasing power-law behavior, as measured by linear fit of the SD variogram scatterplots in double logarithmic space, along a gradient of topographic complexity measured by fractal dimension. Black lines are best-fit non-linear regression lines; red lines are the linear regressions.

**Figure 3:** Near the percolation threshold, power-law behavior appears in the SD variogram in a narrow scaling region. This represents a phase transition between fires whose spread is endogenously controlled and those controlled by exogenous factors. (a) Power-law behavior (linearity in log-log space) is apparent when a lack-of-fit (LOF) test for the linear model is not rejected (p-values between 0.10 and 1.0). A phase transition occurs at  $p_{\text{spread}} \approx 0.495$ . At  $p_{\text{spread}} \geq 0.6$  the LOF test is non-significant but the result is

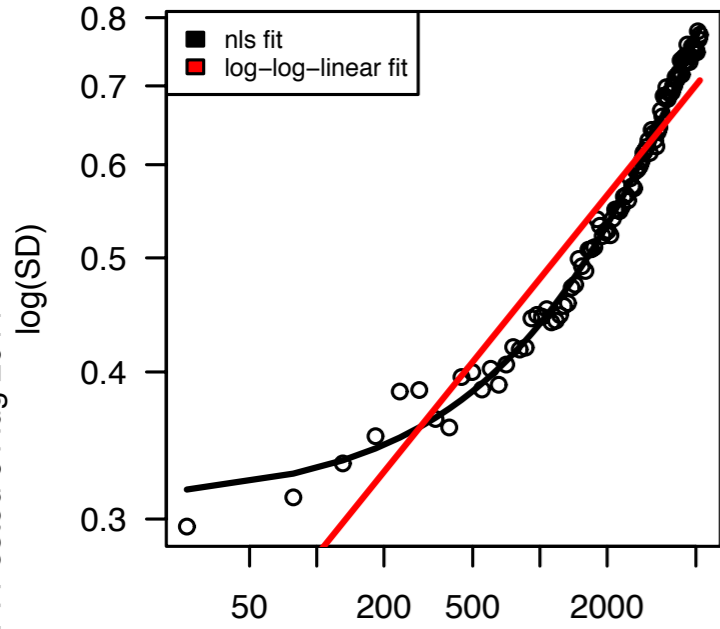
trivial because the slope of the SD variogram is zero. This happens because for this part of the analysis we did not include exogenous controls on fire size. (b) Simulated fire shape with  $p_{\text{spread}}$  well above the percolation threshold (0.57) shows a fire with a regular shape and a lower perimeter:area ratio (c) Simulated fire shape with  $p_{\text{spread}}$  at or just below the threshold (0.49) shows a fire with an irregular shape and a higher perimeter:area ratio.

**Figure 4:** Monte Carlo tests of parameters from the original stochastic model and the SOC model. (a) Distributions of  $p_{\text{spread}}$  that produced SD variograms not significantly different ( $\alpha = 0.25$ ) from real watersheds, based on Monte Carlo simulations described in Methods. With increasing topographic complexity,  $p_{\text{spread}}$  approaches the percolation threshold of 0.495. (b) Distributions of  $\mu_{\text{size}}$  that produced SD variograms not significantly different ( $\alpha = 0.25$ ) from real watersheds. In contrast to  $p_{\text{spread}}$ , the optimal value of  $\mu_{\text{size}}$  is more tightly constrained in watersheds of lower topographic complexity. (c) Distribution of p-values for lack-of-fit tests of the ignition frequency parameter in the SOC model, showing a scaling region of non-significance ( $p > 0.25$ ) for Swauk Creek (complex topography) but not for Twenty Mile, and confirming that the SOC model replicates landscape fire dynamics only in the region of criticality.

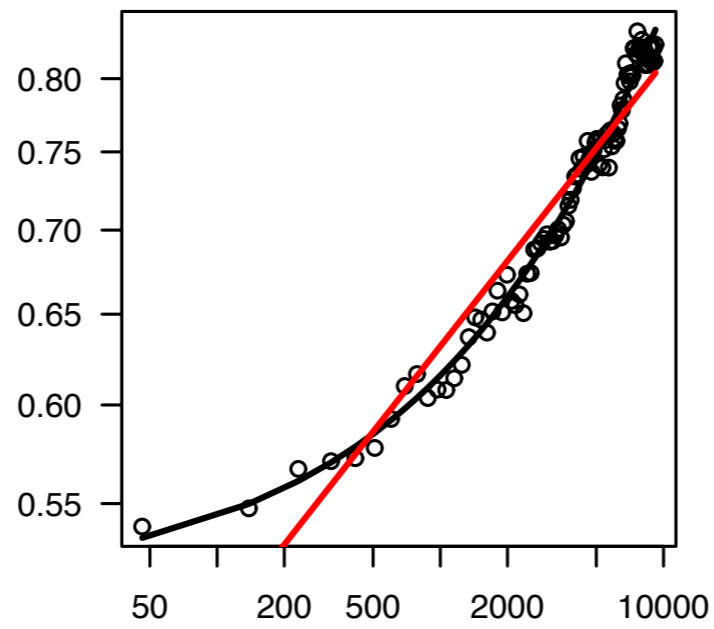


McKenzie & Kennedy -- Figure 1

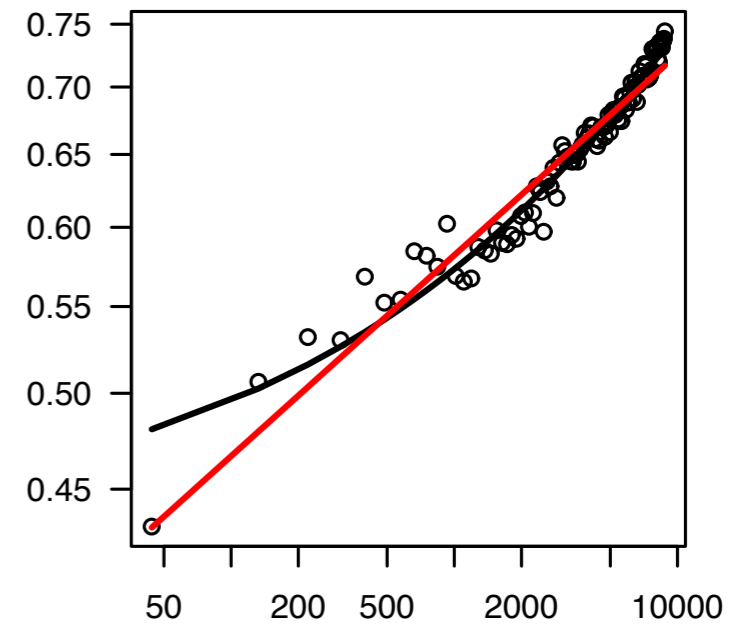
**Twenty Mile**



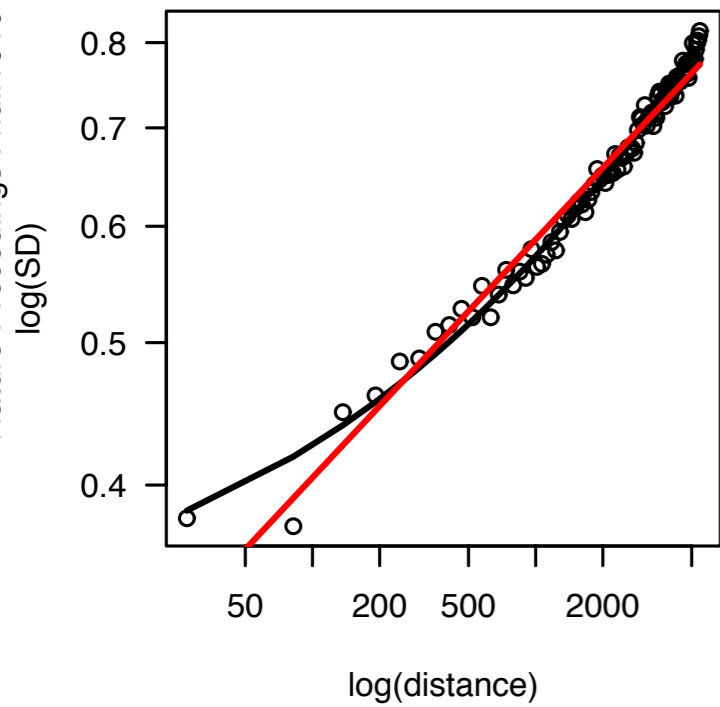
**Frosty Creek**



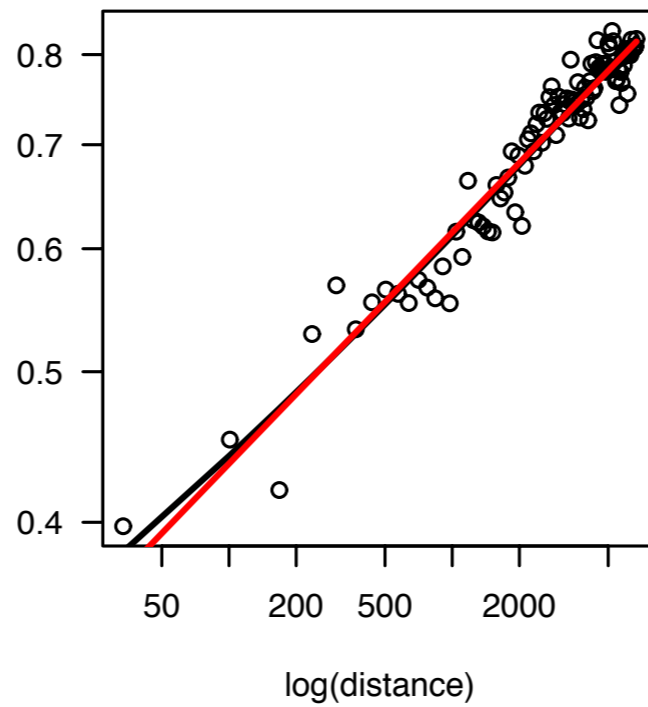
**Entiat**



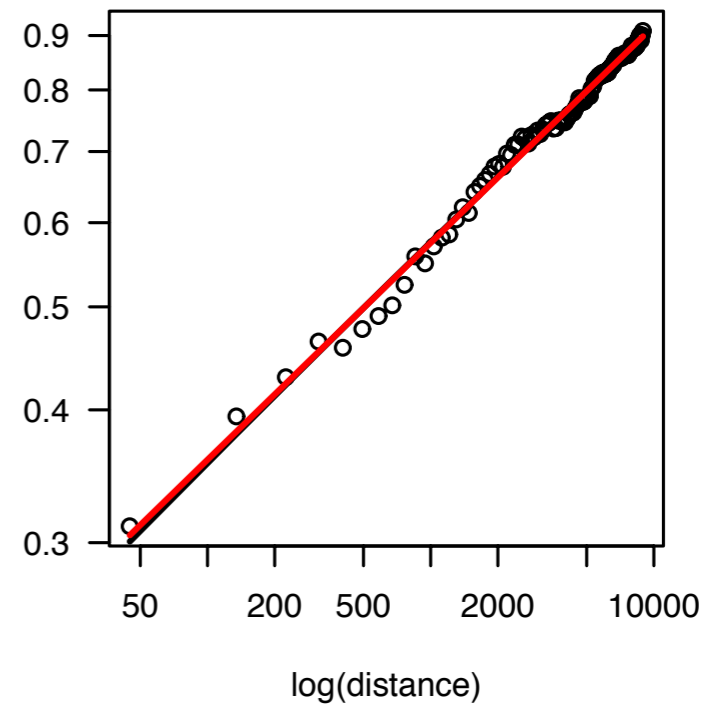
**Nile Creek**

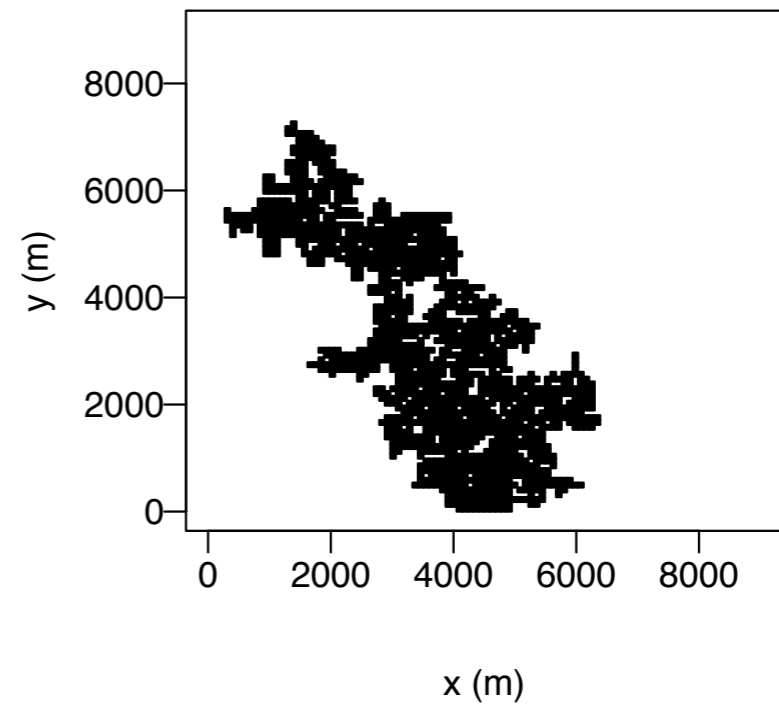
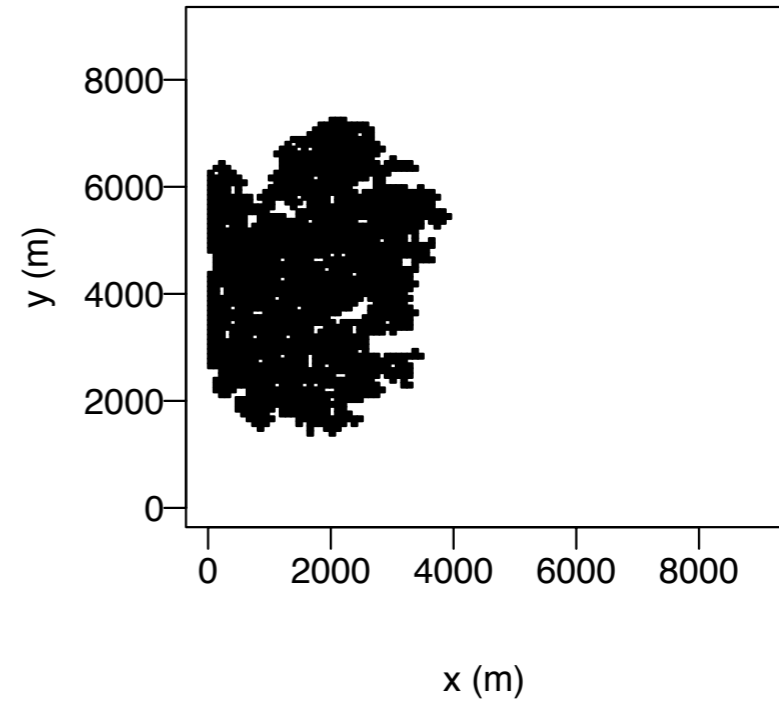
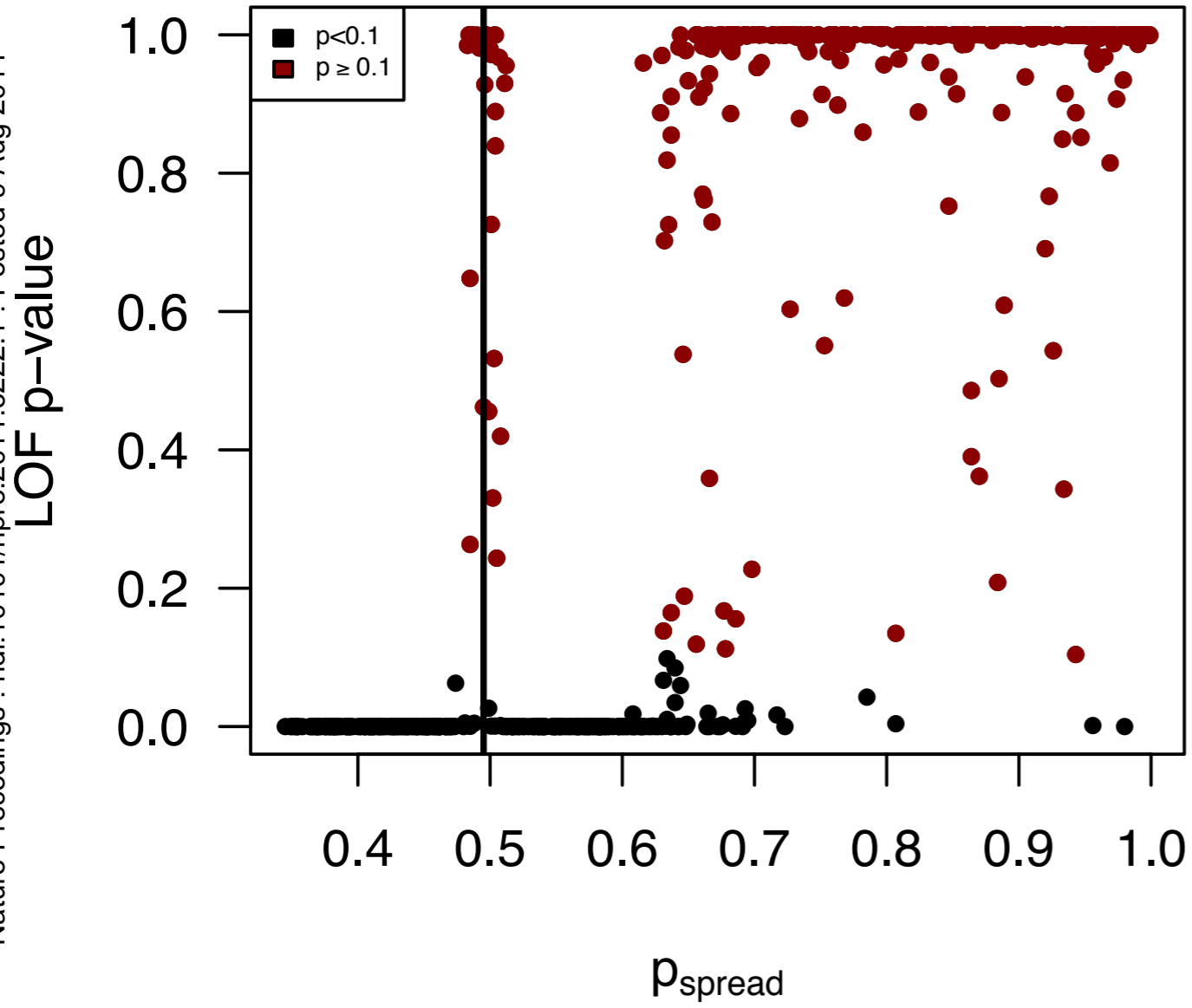


**Quartzite**



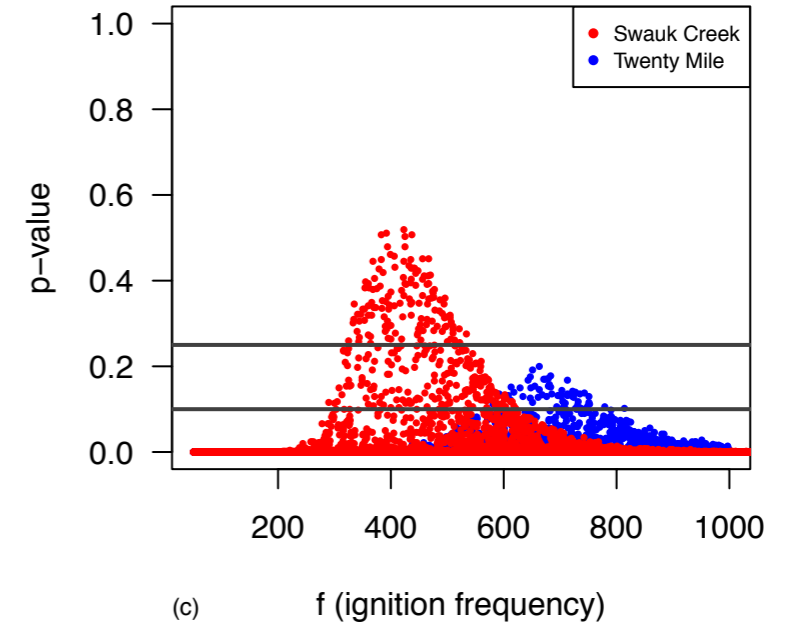
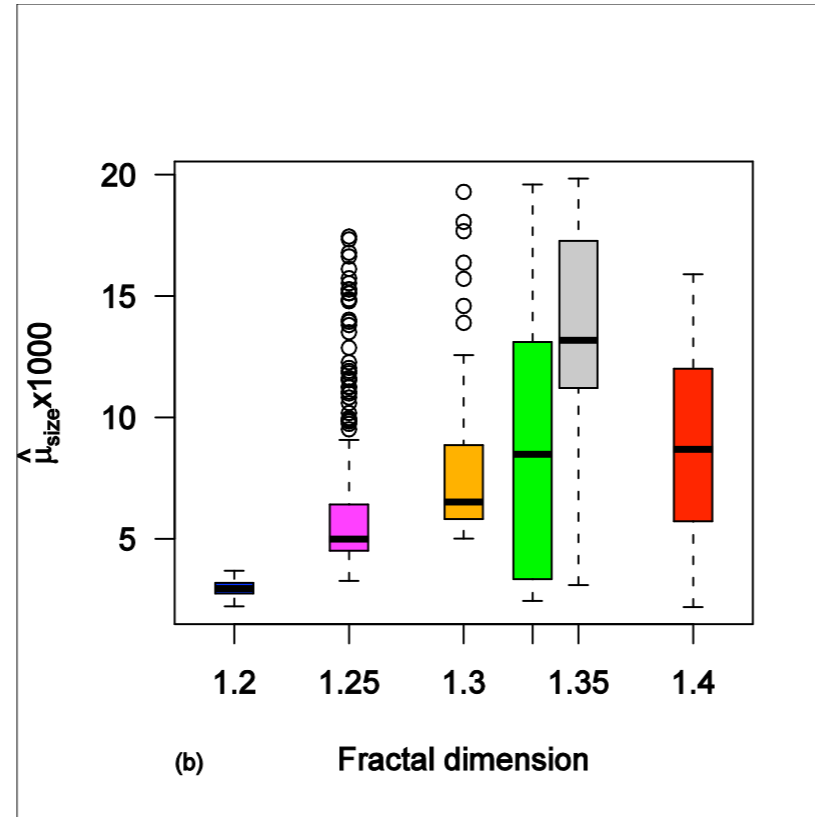
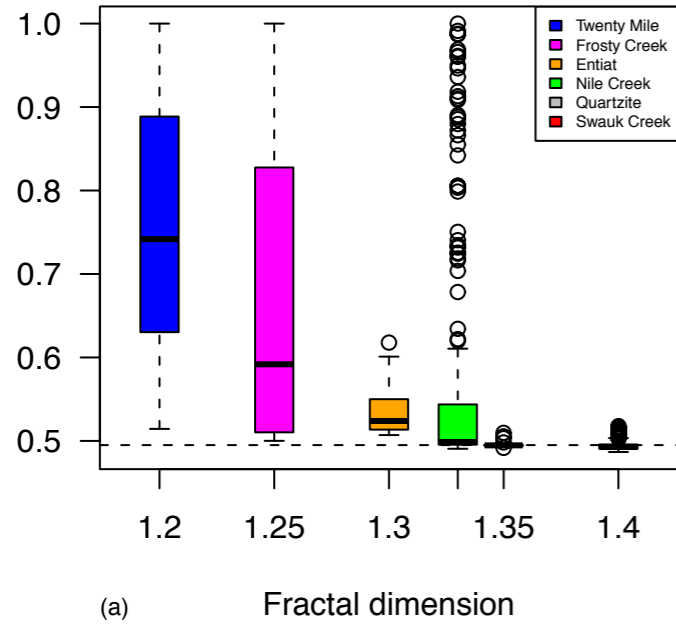
**Swauk Creek**





McKenzie & Kennedy -- Figure 3





McKenzie & Kennedy -- Figure 4

## Supplementary Information

### Fire history data

Fire-history reconstructions in low-severity fire regimes rely on the presence of fire-scarred trees (recorder trees) in a landscape, where the presence of a scar is cross-dated to provide an estimate of the year and sometimes season in which a fire occurred on the landscape. Traditionally these sources of data have been used to calculate aggregate measures such as the fire-return interval, while missing the potential to infer more spatially explicit information possible from the fire-scar data. Our dataset records not only the presence of scars, but also the locations of the recorder trees. This data set provides a marked point pattern of recorder trees, with the marks being the observation of a scar a given year.

### *Fire history matrix*

The fire-history matrix summarizes the scar pattern for a set of recorder trees in a given landscape (Table S1). For each combination of tree and fire year an entry in the matrix is 1 if the tree records that fire, 0 otherwise.

Table S1. Example fire history matrix if there were five fires and seven recorder trees. A zero indicates no scar is recorded for a given tree and fire year, and a one indicates that a scar is recorded for a given tree and fire year.

	Tree						
Fire year	A	B	C	D	E	F	G
Y <sub>1</sub>	0	1	0	0	0	1	1
Y <sub>2</sub>	0	0	0	1	0	0	1
Y <sub>3</sub>	1	1	0	1	1	0	0
Y <sub>4</sub>	1	1	0	0	0	1	0
Y <sub>5</sub>	1	0	1	0	1	1	0

*The Sørensen distance (SD) variogram*

Kellogg et al. (2) exploited the wealth of knowledge made possible with these point patterns by calculating a spatially correlated metric and comparing the spatially correlated patterns among the fire history sites. First they calculated the Sørensen distance (SD) for every pair of recorder trees on a given landscape. The SD is a metric commonly used in community ecology to measure species co-occurrence. It is calculated from a frequency table that compares the fire history of two recorder trees (Table S2; equation S1).

Table S2. Frequency table summarizing the fire history of two trees (A and B).  $n_{11}$  is the number of years both trees record a fire,  $n_{10}$  is the number of years A records a fire but B does not,  $n_{01}$  is the number of years B records a fire but B does not and  $n_{00}$  is the number of years neither tree records a fire. Numbers in each cell are taken from the example fire history presented in Table 1.

	A=1	A=0
B=1	$n_{11}=2$	$n_{01}=1$
B=0	$n_{10}=1$	$n_{00}=1$

$$SD = 1 - \frac{2n_{11}}{2n_{11} + n_{10} + n_{01}} \quad (S1)$$

SD can take continuous values on the range (0,1), with zero indicating completely similar fire histories between a pair of trees and one indicating completely dissimilar fire histories between a pair of trees. In the example from Tables S1 and S2, the value of SD for the pair A and B is 0.33, indicating a relatively similar fire history for that pair.

Kellogg et al. (2) produced what they termed Sørensen variograms by binning the

between-tree pair-wise distances, calculating the mean SD for all pairs of trees for a given distance bin, and plotting the mean SD against distance.

Kellogg et al. (2) also calculated the fractal dimension for each landscape as a surrogate for topographic complexity. This metric relates to the average standard deviation of elevation with increasing window lengths as a moving average, and the fractal dimension increases with topographic complexity. They found that the fire-history sites formed a gradient of topographic complexity and that the shape of the associated SD variogram also varied along that gradient.

### **Neutral model for fire history**

We use the neutral model for fire history presented by Kennedy and McKenzie (3) to determine whether observed patterns in fire history data can be replicated by simple stochastic processes. See Kennedy and McKenzie (3) for a detailed description and evaluation of the model. After it is initialized, the neutral model emulates two major processes: fire spread and recorder tree scarring.

#### *Initialization*

The neutral model is initialized with a blank raster grid with 100x100 pixels. A point pattern of complete spatial randomness (CSR) recorder trees is overlain on the raster grid and retained throughout the simulated fire history. These are the trees available for scarring and fire spread is independent of the presence of recorder trees. The number of fires simulated for an individual is a random number determined by

sequential draws from an exponential distribution. First a mean fire-return interval is specified (we use 3 years) and a random number of years between fires is drawn from the exponential distribution with that mean fire return interval. This is repeated until the first draw at which the cumulative sum of fire-return intervals is  $\geq 200$ . The number of random draws determines the number of fires to be spread. For each fire in the history a random fire size expressed as the number of pixels burned is drawn from a gamma distribution whose mean is a mean fire size ( $\mu_{size}$ ).

### *Fire spread*

For each fire an ignition point on the raster grid is randomly chosen, with a five-cell buffer excluded along the edge. Fire spreads iteratively from the ignition point according to a simple probability test ( $p_{spread}$ , Figure S1). For each of the four orthogonal neighbors (up, down, left and right) a random number is drawn from a uniform (0,1) distribution. If the random number is  $\leq p_{spread}$ , then fire spreads to that neighboring pixel. Once all four tests of fire spread are conducted the initial pixel can no longer spread fire for that fire in the history.

In the next iteration the four neighbors for each pixel burned in the previous iteration are tested for spread as before. For each fire in the history this process is iterated until one of three stopping points is reached. 1) if all tests of spread fail in a given iteration the fire can no longer spread and the next fire is initialized (the fire burns out on its own). 2) if the number of pixels burned in the current fire  $\geq$  the random fire size then fire spread is halted and the next fire is initialized. 3) if the fire spreads to each

of the four borders of the raster grid fire spread is halted and the next fire is initialized. Each fire is spread independently of the previous fires so there is no memory in the landscape process.

### *Recorder tree scarring*

Recorder trees are tested for scarring when a fire reaches a pixel occupied by  $\geq 1$  recorder tree. For each recorder tree in a burned pixel a random number is drawn from a uniform (0,1) distribution and if the random number is  $\leq$  the probability of scarring ( $p_{scar}$ ) a scar is recorded for that tree for that fire. Scarring is independent tree-tree and fire-fire.

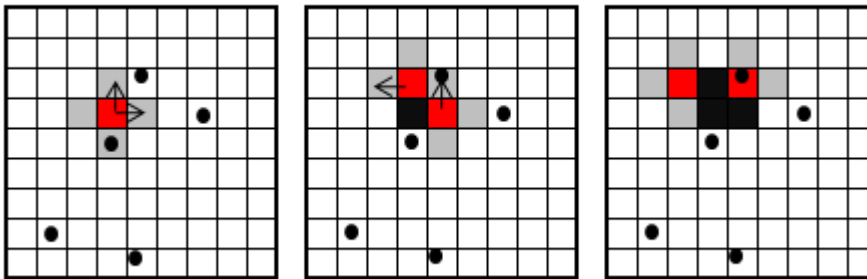


Figure S1. Initialization and second iteration of fire spread in the neutral model for fire history. For illustration a small raster grid is shown. Black dots indicate recorder trees scattered randomly across the raster grid. Red pixels are actively spreading fire. Fire spread is initialized with a randomly drawn ignition point (red pixel), and from that pixel each of the four neighbors is tested for fire spread (grey pixels) against the spread probability ( $p_{spread}$ ). In this example the ignition point successfully spreads forward and to the right (black arrows). Once fire is tested for spread from a burning pixel then that pixel can no longer spread fire (indicated by a black pixel). In the second iteration the neighbors of the newly ignited pixels are tested for spread. Note that if a pixel neighbors two burning pixels it is tested twice for fire spread. Already burned pixels are not tested again for spread. If a burned pixel is occupied with a recorder tree that tree is tested for scarring only in the iteration fire spreads to it.

*Model outputs*

The structure of the neutral model enables us to calculate simulated fire-history matrices and SD variograms for varying combinations of neutral model parameters. We can then compare simulated SD variograms to observed and use the neutral model structure to derive an expectation for SD for a given pair of recorder trees.

**Deriving an expectation for Sørensen's distance (SD)**

Kennedy and McKenzie (3) use the probability structure of the neutral model to derive an expectation for the value of SD between a given pair of recorder trees (A and B). They first derived expectations for each cell in the frequency table (Table S3), then combined those into equation S1.

Table S3. Expected values for each cell in the frequency table that summarizes the fire history of two trees (A and B; taken from Kennedy and McKenzie (3)).  $k$  is the number of fires in the fire history,  $A_{\text{fire}}$  is the event that tree A experiences a fire,  $B_{\text{fire}}$  is the event that tree B experiences a given fire,  $p_{\text{scar}}$  is the probability a tree records with a scar a fire that it experiences, and  $P(B_{\text{fire}}|A_{\text{fire}})$  is the probability that tree B experiences a fire given tree A has experienced that fire.

	A=1	A=0
B=1	$E(n_{11}) = k * P(A_{\text{fire}}) * P(B_{\text{fire}} A_{\text{fire}}) * p_{\text{scar}}^2$	$E(n_{01}) = k * P(A_{\text{fire}}) * p_{\text{scar}} * [1 - P(B_{\text{fire}} A_{\text{fire}}) * p_{\text{scar}}]$
B=0	$E(n_{10}) = k * P(A_{\text{fire}}) * p_{\text{scar}} * [1 - P(B_{\text{fire}} A_{\text{fire}}) * p_{\text{scar}}]$	

Kennedy and McKenzie (3) show through simple algebraic manipulations that when combined, the complicated equations reduce to a simple expression for the expected value of SD.

$$E(\text{SD}) = 1 - p_{\text{scar}} P(B_{\text{fire}}|A_{\text{fire}}), \quad (\text{S2})$$

where  $P(B_{\text{fire}}|A_{\text{fire}})$  is the probability a second tree (B) experiences fire given the first tree (A) has experienced fire. This probability depends on the spatial structure of the fire and the fire size, which change with the model parameters  $p_{\text{spread}}$  and  $\mu_{\text{size}}$  (3).

### **Self-organized criticality (SOC) model with fire scars**

We programmed an SOC forest fire model (Figure S2) after (6) and overlaid a CSR pattern of recorder trees on the SOC grid. The SOC model is initialized with a blank raster grid. Each iteration fuel is dropped randomly on the grid, with each pixel having an equal chance to receive fuel. If the random pixel is already occupied with fuel the model continues to the next iteration. The parameter of the SOC model is the frequency of sparks that are dropped onto the SOC grid ( $f$ ). Every  $f$  iterations a spark is dropped, with each pixel having an equal chance for sparking. If the random pixel chosen for the spark is occupied with fuel then it and every neighboring pixel also occupied with fuel is ignited (Figure S2). In our modified model fuel accumulation and sparking are independent of the presence of recorder trees, which occupy a given pixel throughout the simulated fire history. If a pixel included in the SOC fire is occupied by a recorder tree, then that tree is tested for scarring as in the neutral model. Our modified SOC model then has two parameters: frequency of sparks ( $f$ ) and probability of scarring ( $p_{\text{scar}}$ ).



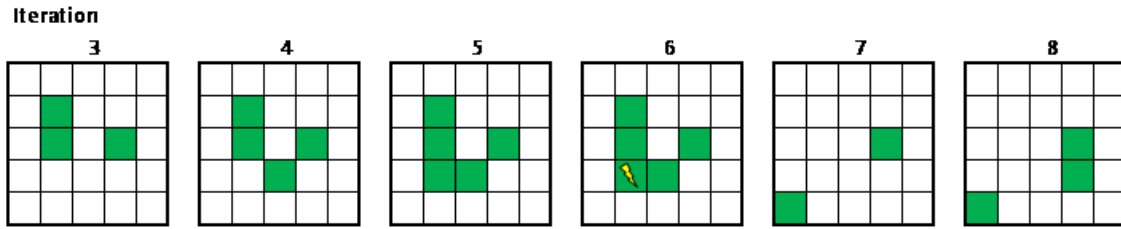


Figure S2. Simple schematic of an SOC model on a small grid, showing iterations 3 through 8. In subsequent iterations fuel is dropped onto the raster grid (occupied cells are green). At a fixed iteration ( $f=6$  in this example) a spark is dropped on the raster grid (yellow lightning). If the spark hits an unoccupied cell then nothing happens. If that spark hits an occupied cell then it and every neighboring cell is ignited and removed from the grid. In the next iterations after a spark is dropped fuel is again dropped randomly until the next spark is dropped.